Advanced High-Temperature CO2 Sorbents with Improved Long-Term Cycling Stability

ACS APPLIED MATERIALS & INTERFACES

Energy, Environmental, and Catalysis Applications

Advanced high temperature CO2 sorbents with improved long-term cycling stability

Nityashree Nagesh, Manohara Gudiyor Veerabhadrappa, M. Mercedes Maroto-Valer, and Susana Garcia

ACS Appl. Mater. Interfaces, **Just Accepted Manuscript** • DOI: 10.1021/acsami.0c08652 • Publication Date (Web): 01 Jul 2020

Just Accepted

is published by the American Chemical Society. 1155 Sixteenth Street N.W., Washington, DC 20036

Advanced high temperature CO_2 sorbents with improved long-term cycling stability

N. Nityashree, G. V. Manohara, M. Mercedes Maroto-Valer, S. Garcia*

Research Centre for Carbon Solutions (RCCS), School of Engineering and Physical Sciences, Heriot-Watt University, Edinburgh EH14 4AS, United Kingdom.

Corresponding author: s.garcia@hw.ac.uk (S. Garcia)

Abstract

Developing novel sorbents with maximum carbonation efficiency and good cycling stability for CO_2 capture is a promising route to sequester anthropogenic CO_2. In this work, we have employed a green synthesis method to synthesize CaO based sorbents suitably stabilised by MgO and supported by *in situ* generated carbon under inert atmosphere. The varied amounts (10 - 30 wt %) of MgO were used to stabilize the CaO. The supported mixed metal oxide (MMO) sorbents were screened for high temperature CO_2 capture under CO_2 rich (86 % CO_2) and lean (14 % CO_2) gas streams at 650 °C and atmospheric pressure. The MMO sorbents captured 53 to 63 wt % of CO_2 per gram of sorbent under 86 and 14 % CO_2, respectively, accounting for about 98 % carbonation efficiency, which outperforms the CO_2 capture capacity of limestone derived CaO (L-CaO) sorbents (22.8 wt %). All the synthetic MMO sorbents showed greater capture capacity and cyclic stability when compared to benchmark L-CaO. Due to the high carbonation efficiency and cycling stability of g-$Ca_{0.69}Mg_{0.3}O$ sorbent, it was tested for 100 carbonation/regeneration cycles of 5 min each under CO_2 lean conditions. The g-$Ca_{0.69}Mg_{0.3}O$ sorbent showed exceptional CO_2 capture capacity and cycling stability and retained about 65 % of its initial capture capacity after 100 cycles.

Keywords: High temperature CO_2 capture, carbon supported MMO sorbents, carbonation efficiency, cyclic carbonation/regeneration, calcium oxide, magnesium oxide.

1. Introduction

Carbon dioxide capture, utilisation and storage (CCUS) is a promising approach for reducing emitted CO_2 amounts and consequently, minimising the adverse effects of global warming[1,2]. Efficient CO_2 capture is critical for subsequent CO_2 storage or utilisation technologies[3]. Unfortunately, the current CO_2 capture technologies involving liquid amines are costly and present environmental concerns[4]. In contrast, the adsorption of CO_2 using solid based sorbents is a sustainable alternative to liquid amines[5]. Solid sorbents have significant advantages such as ease of preparation and handling, tuneable and variable compositions, better heat capacities / lesser regeneration penalties and operate over a wide temperature range (room temperature to 700 ˚C)[6]. Various solid sorbents such as metal oxides (MO)[7], mixed metal oxides (MMO)[8], porous crystalline materials[9], zeolites[10] and porous carbons[11] have been employed for CO_2 capture. MO and MMO have advantage over other solid sorbents as they work well at the temperatures at which CO_2 is emitted from various industrial sources (such as, cement, iron and steel and coal fired power plants)[12]. CaO is very attractive amongst the MO as a high temperature CO_2 sorbent as it is abundant, environmentally benign and inexpensive[13]. Intrinsic structure, morphology and thermal/mechanical stability of CaO are fundamentally decisive for efficient CO_2 capture[14]. However, benchmark limestone-based CaO sorbents (L-CaO) lose their CO_2 capture capacity and cycling stability quickly due to sintering[15]. To overcome the limitations of L-CaO, a number of synthetic CaO-based sorbents were synthesized[14]. Synthetic CaO sorbents were prepared by different synthesis methods[16], varied experimental conditions[17] and by employing different starting precursors[18,19]. The CO_2 capture performance of synthetic CaO was found to be better than L-CaO[19]. However, the CO_2 cycling stability of these materials needed further improvement. To improve the thermal/mechanical stability and long-term cycling stability of CaO sorbents, various dopants or supports such as alumina[20], zirconia[21], magnesia[22], silica[23], yttrium oxide[24], titanium oxide[25], etc., have been used. Finally, a few carbon-based inert supports have also been reported to improve the stability of CaO sorbents[26,27]. Due to the beneficial effect of the carbon support on the stability and activity of the materials, many mesoporous / microporous carbon supported materials are used for various applications[28–30]. Carbon composited with active CO_2 capturing materials have shown a positive effect on CO_2 capture properties of the sorbents[26,27,31,32]. The carbon support is

expected to offer mechanical and thermal stability to the sorbents increasing its CO_2 capture capacities and cycling stabilities of sorbents[28].

Conventionally, synthesis of doped CaO is achieved via solid state reactions[33], molten-salt synthesis[34], chemical vapour deposition[35], spray pyrolysis[36], sol-gel synthesis[37], solution combustion[38] or by physically mixing the dopant with the CaO[39]. Generally, these methods are energy intensive, need specialised set-up and are multi-step. Therefore, it is important to develop simple and eco-friendly methods for preparing doped CaO by using simpler preparation techniques[40]. Homogeneous precipitation method is known to give solid solutions with uniform compositions[41]. Among all the dopants used to stabilise CaO sorbents, MgO is an attractive candidate due to its abundance, non-toxicity and cost. Additionally, MgO has also been used for CO_2 capture and it shows around 5 wt % CO_2 capture in the temperature range of 200–300 °C[42]. Several MgO stabilised CaO sorbents with interesting structure and morphology, synthesised by different procedures, were reported recently[19]. The presence of MgO induced structural stability to CaO resulting in better CO_2 capture capacities and cycling stabilities[43]. The MgO is known to increase the distance between CaO particles preventing CaO from sintering during repeated cycles of carbonation and regeneration[26,44]. Since MgO has a high Tammann temperature of 1150 °C in contrast to $CaCO_3$ which is 533 °C, it acts as a barrier and prevents the sintering of $CaCO_3$[22]. However, there is further scope to improve the synthesis method, capture and long-term cycling stability of the MgO doped CaO that would make them promising materials to employ for industrial scale CO_2 capture. Layered metal hydroxides and hydroxy salts provide ample opportunity to design precursor materials for mixed metal oxides (MMO) of desired composition with homogeneous distribution of metal ions. Recently, layered hydroxysalts / layered double hydroxides are prepared in an eco-friendly manner by employing metal hydroxides as starting materials for CO_2 capture[45]. The controlled thermal decomposition of the metal hydroxide precursors resulted in the formation of carbon stabilized MO and MMO[46]. Here we have employed a similar eco-friendly synthesis approach to develop a single precursor for MgO stabilized CaO supported on *in situ* generated carbon support. The Ca/Mg ratio was varied in the precursor hydroxysalts to get different amounts of CaO and MgO. The synthesized Ca/Mg-hydroxysalt precursors were decomposed under inert atmosphere to get carbon supported MgO stabilised CaO sorbents. The sorbents were tested for CO_2 capture capacity and cycling stability under CO_2 rich (86%) and lean (14%) conditions.

2. Synthesis and Characterization

2.1. Preparation of Ca, Mg - adamantanecarboxylate precursors

All chemicals, $Ca(OH)_2$, $Mg(OH)_2$ and 1-adamantanecarboxylic acid were purchased from Sigma Aldrich and used as received. Deionised water (18.2 MΩ.cm resistivity, Millipore water purification system) was used throughout the synthesis. 1-adamantanecarboxylate salts of Ca and Mg in different mole ratios (Ca : Mg = 90 : 10, 80 : 20 and 70 : 30) were synthesized by the co-hydration method[26]. Typically, stoichiometric amounts of $Ca(OH)_2$, $Mg(OH)_2$ and 1-adamantanecarboxylic acid [(Ca+Mg) : adamantanecarboxylate = 1 : 2] were suspended in 100 mL water. The reaction mixture was stirred at room temperature for an hour to get a homogeneous mixture. The resultant reaction mixture was transferred to a Teflon-lined vessel and hydrothermally treated at 150 °C for 24 h. The resultant samples were recovered by filtration and dried at 75 °C overnight.

2.2. Preparation of carbon supported MMO sorbents

The carbon supported Ca and Mg MMO sorbents were synthesized by decomposing each of the Ca, Mg - adamantanecarboxylate precursors under inert atmosphere using N_2. About 1.0 g of each of the as prepared precursor samples were loaded into a quartz tube and subjected to decomposition at 700 °C under N_2 atmosphere (N_2 flow rate of 100 mL/min, ramp rate 10 °C/min, residence time 2 h). A limestone sample procured from British Geological Society (BGS) was also subjected to decomposition under identical conditions to get L-CaO sorbent for comparison.

2.3. Characterization

Powder X-ray Diffraction (PXRD) patterns were obtained using a Bruker D8 Advance power diffractometer with Ge-monochromated Cu-Kα1 radiation (λ = 1.5406Å) from a sealed tube, operating at 40kV and 40mA with a Lynx Eye linear detector in reflectance mode. Data was collected over angular range of 2-70 °2θ with a step size of 0.009˚ over half an hour. Fourier Transform Infrared spectra (FTIR) of the samples were acquired using a Perkin Elmer spectrometer in ATR mode (4000 to 400cm^{-1}). Elemental analysis of Ca^{2+} and Mg^{2+} (ICP-OES) was carried out by atomic emission technique using a Perkin Elmer Optima 5300DV. 1 N nitric acid was used to dissolve 100 mg of each sample after decomposition at 700 °C in air for 2 hours. The ICP-OES analysis was run in duplicates in order to estimate the Ca : Mg

ratios. The C, H and N analysis of the precursor samples and the MMO sorbents was carried out by taking approximately 3 mg of sample that was placed in a tin capsule and combusted in a high oxygen environment at 950 °C using an Exeter Analytical CE-440 elemental analyser calibrated with acetanilide. Surface area analysis of the MMO sorbents was carried out by gas adsorption technique (N_2, 77 K) using a Micromeritics Gemini VII2390 V1.03 instrument. Prior to the gas adsorption measurement, the sample was degassed for 5 h at 100 °C. Surface area and pore diameter were calculated by BET method and pore volume was calculated by DFT method. The surface morphology of the sample was also characterized by FEI Scios scanning electron microscopy (SEM) using ETD secondary electron detector at 5kV. EDX mapping was performed at an electron beam acceleration of 10 kV using EDAX Octane Plus detector.

2.4. CO_2 capture studies

Thermal analysis and CO_2 capture studies were performed using a thermogravimetric analyser (TA Instruments TA 500). Precursor samples were used instead of preformed MMO to avoid any contamination from atmospheric CO_2. The precursor samples were loaded onto a platinum pan and decomposed under inert atmosphere (using 100 mL/min N_2, 2 h, 700 °C, 10 °C/min). The temperature then was brought to the desired capture temperature and CO_2 gas was switched on (for 2 h) to test the uptake capacity of the resultant carbon supported CaO-MgO MMO sorbents. Cyclic CO_2 capture capacity of the sorbents was evaluated and compared with L-CaO sorbent under similar conditions. For the cyclic experiments, all samples were heated at a rate of 10 °C/min under a flow of nitrogen gas (100 mL/min) up to 700 °C and kept isothermal for 2 hours in order to generate the corresponding MMO sorbent. The samples were cooled to 650 °C and then equilibrated with CO_2 rich (86 % volume/N_2 balance) gaseous mixture for 30 minutes for CO_2 sorption (carbonation). The carbonated samples were then regenerated by heating to 700 °C at 10 °C/min and keeping isothermal for 30 minutes under a flow of nitrogen gas (100 mL/min) to regenerate the oxide. Ten cycles of carbonation-regeneration were conducted to screen the materials. Similar experiments were repeated with a CO_2 lean gaseous mixture that contained 14 % CO_2 (N_2 balance) for ten cycles. The long-term cycling stability (100 cycles) of the best performing sorbent, identified based on its working capacity (with respect to amount of CaO present) and performance consistency, was investigated over cycles of shorter carbonation/regeneration duration (5 min) under CO_2 lean conditions (14 % CO_2).

3. Results and Discussion

3.1. Sample characterization

Three compositions (Ca : Mg = 90 : 10, 80 : 20 and 70 :30) of Ca, Mg -adamantanecarboxylate precursors were prepared using a green method. The metal hydroxide mixtures were hydrothermally treated with twice the number of moles of 1-adamantanecarboxylic acid in water, as described in the experimental section. The as prepared precursor samples were separated from the supernatant by filtration, dried and used without further processing according to a recent report[26]. The composition of the as synthesized Ca, Mg -adamantanecarboxylate precursors was calculated based on CHN and ICP-OES analysis. Both, estimated and expected weight percentages, along with the mole ratios of Ca and Mg for the three precursors are shown in Supporting Information (SI), Table S1. The observed Ca : Mg mole ratios were 8.95 : 1, 3.97 : 1 and 2.30 : 1 as opposed to the expected ratios of 9 : 1, 4 : 1 and 2.33 : 1, respectively, for the three precursors. C and H percentages listed in SI, Table S1 indicate a good agreement between the observed and expected C content in the precursors. However, slightly higher values for H were observed for all the precursors which could be due to adsorbed/crystallised water molecules. The empirical formulas deduced for the precursors were $Ca_{0.89}Mg_{0.1}$ $(Ada)_{1.98}\cdot 1.2$ H_2O, $Ca_{0.79}Mg_{0.2}$ $(Ada)_{1.99}\cdot 1.3$ H_2O and $Ca_{0.69}Mg_{0.3}$ $(Ada)_{2.01}\cdot 1.4$ H_2O (SI, Table S1), hereafter referred to as $Ca_{0.89}Mg_{0.1}$-Ada, $Ca_{0.79}Mg_{0.2}$-Ada and $Ca_{0.69}Mg_{0.3}$-Ada, respectively.

The functional groups present in the precursor samples were identified by using FTIR spectroscopy. The FTIR spectra of $Ca_{0.89}Mg_{0.1}$-Ada, $Ca_{0.79}Mg_{0.2}$-Ada and $Ca_{0.69}Mg_{0.3}$-Ada are shown in SI, Figure S1a, b and c, respectively. The presence of adamantanecarboxylate ion is indicated by the asymmetric and symmetric stretching vibrations due to carboxylate ion at about 1350 and 1550 cm^{-1}, respectively[47]. A split in the peak is due to the M^{2+}-carboxylate bonding in the samples[47]. Peaks due to all-trans C-H stretching vibrations[47] are seen at around 2850 and 2950 cm^{-1}. A broad hydrogen bonded O-H stretching vibration due to adsorbed water was seen at about 3400 cm^{-1} in all the samples[47].

PXRD patterns of the $Ca_{0.89}Mg_{0.1}$-Ada, $Ca_{0.79}Mg_{0.2}$-Ada and $Ca_{0.69}Mg_{0.3}$-Ada precursor samples are shown in SI, Figure S2a, b and c, respectively. All samples show similar patterns with distinct diffraction peaks at 2θ, 6.26°, 6.80°, 11.19°, 13.54°, 16.22°, 17.51° and 24.72°

corresponding to *d*-spacing values of 14.10 Å, 12.98 Å, 7.90 Å, 6.53 Å, 5.46 Å, 5.06 Å and 3.59 Å, respectively. 100 % intensity peak of all the samples appear at 12.98 Å. Reflections of the Ca, Mg -adamantanecarboxylate precursors are similar to the previously reported metal-adamantanecarboxylate samples[26,46]. Reflections due to unreacted metal hydroxides that are expected at *d*-values of 4.6 Å and 2.3 Å were absent, indicating the absence of unreacted metal hydroxide in the precursor samples.

Carbon supported Ca and Mg MMO sorbents were prepared by decomposing the $Ca_{0.89}Mg_{0.1}$-Ada, $Ca_{0.79}Mg_{0.2}$-Ada and $Ca_{0.69}Mg_{0.3}$-Ada precursors in a quartz tube under N_2 gas flow, as described in the experimental section. The resultant MMO sorbents are referred to as g-$Ca_{0.89}Mg_{0.1}O$, g- $Ca_{0.79}Mg_{0.2}O$ and g-$Ca_{0.69}Mg_{0.3}O$, respectively. 'g' indicates disordered graphitic carbon support that was generated *in situ* during decomposition. PXRD patterns of the freshly decomposed samples under N_2 for 2 hours (Figure 1) shows reflections due to the carbon, CaO and MgO. The diffraction peak observed at around 18° 2θ is due to the graphitic carbon support[48] and it was found in all the MMO samples. The graphitic carbon could the remnant carbon left in the MMO sorbents formed due to incomplete degradation of the metal-adamantanecarboxylate precursors under N_2 atmosphere. Diffraction peaks of CaO are observed at 2θ values of 32.23°, 37.42° (100% intensity peak) and 53.84°. Peaks due to MgO phases are observed at 2θ values of 28.77°, 34.14° (100% intensity peak), 42.95°, 50.96° and 62.31°. The relative intensities of the CaO diffraction peaks seem to decrease with increasing concentration of magnesium in the precursors, as seen in Figure 1.

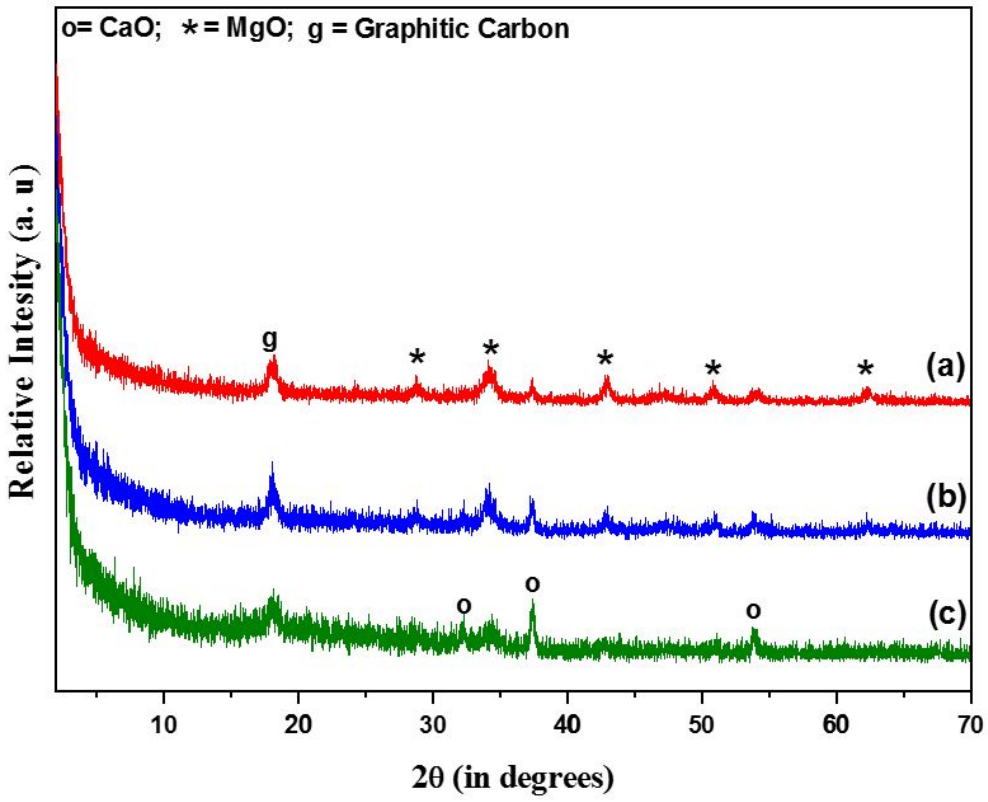

Figure 1. Freshly prepared g-$Ca_{0.89}Mg_{0.1}O$ (a), g-$Ca_{0.79}Mg_{0.2}O$ (b) and g-$Ca_{0.69}Mg_{0.3}O$ (c) samples by decomposition under N_2 at 700 °C for 2 hours.

The morphology of the freshly prepared MMO sorbents was studied using SEM and the images are shown in Figure 2. All MMO sorbents showed micron sized particles (around 10 μm) with a highly porous structure that could be formed due to the templating effect of the *in situ* generated carbon support. The sorbents' images under higher magnifications (Figure 2 b, d and f), illustrate carbon supported polyp-like colonies of MMO formed due to decomposition of the precursor samples. The size of the globules in the freshly decomposed oxide samples decreases with increasing amounts of magnesium, indicating that amount of magnesium in the precursor has on effect on the morphology of the resultant MMO. Earlier reports have shown that CaO of smaller sizes and porous morphology have revealed better regeneration ability of the sorbent for CO_2 capture[49].

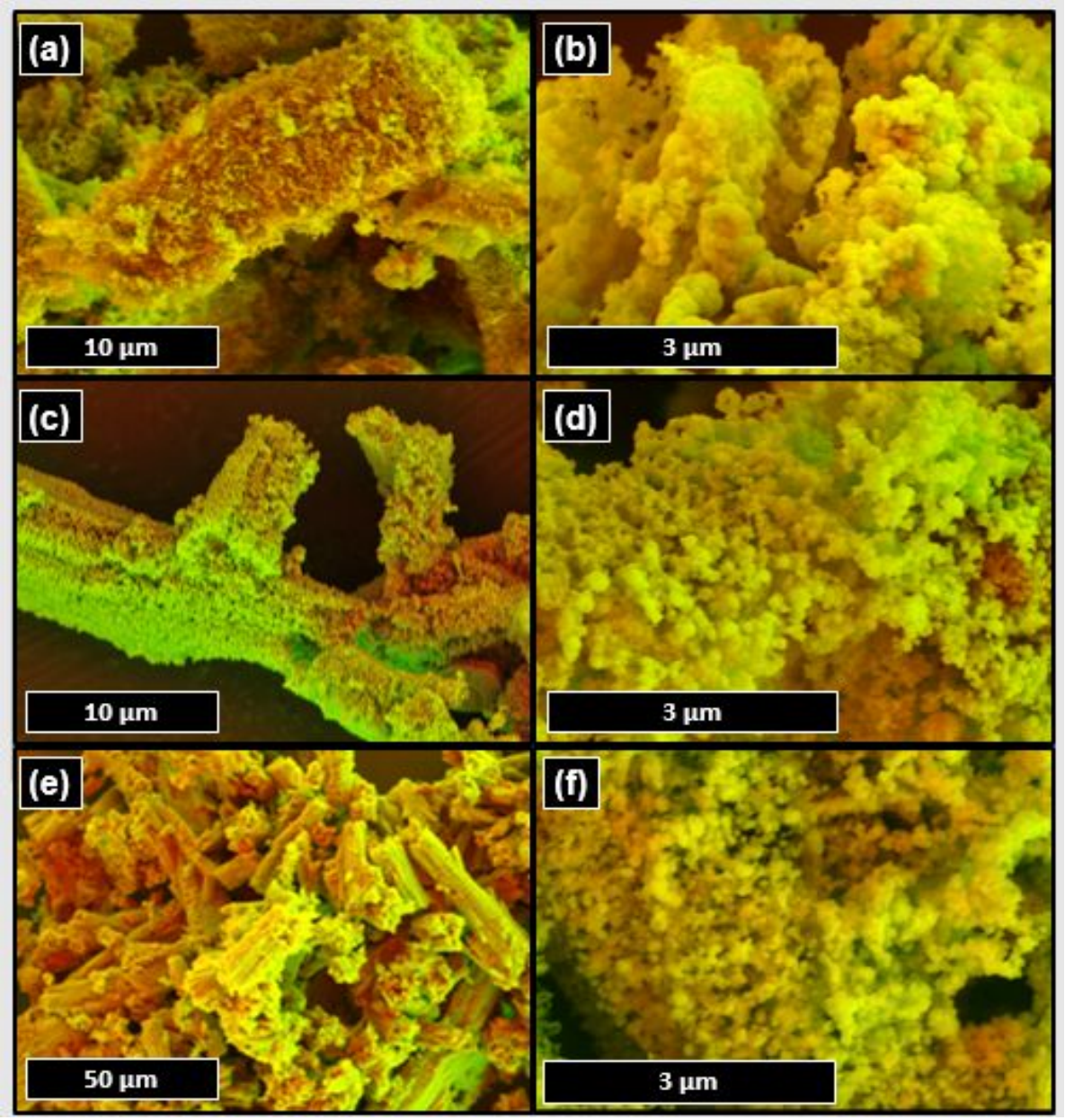

Figure 2. SEM images of freshly prepared g-$Ca_{0.89}Mg_{0.1}O$ (a and b), g-$Ca_{0.79}Mg_{0.2}O$ (c and d) and g-$Ca_{0.69}Mg_{0.3}O$ (e and f) samples obtained after decomposition at 700 °C under N_2 for 2 hours. Scalebars redrawn for clarity.

To further understand the distribution of carbon, magnesium, and calcium in the g-$Ca_{0.89}Mg_{0.1}O$, g-$Ca_{0.79}Mg_{0.2}O$ and g-$Ca_{0.69}Mg_{0.3}O$ sorbents, MMO were mapped using SEM elemental mapping (as shown in SI, Figure S4, S5 and S6, respectively). Uniform distribution of all the elements (except magnesium) was observed. g-$Ca_{0.89}Mg_{0.1}O$ and g-$Ca_{0.79}Mg_{0.2}O$ sorbents showed segregated islands of Mg (SI, Figure S4 and S5 respectively), in contrast to

g-$Ca_{0.69}Mg_{0.3}O$ sorbent (SI, Figure S6) that presented the best distribution of Mg amongst all the sorbents.

The porous texture and surface area of the MMO sorbents were characterized by gas adsorption technique as indicated in the experimental section. Surface area and pore diameter were calculated by BET method and pore volume was calculated by DFT method (values listed in Table 1). All the samples showed type II adsorption isotherms according to the IUPAC system of classification (SI, Figure S3)[50] characteristic of nonporous or macroporous adsorbents. However, the average pore diameters calculated using DFT method indicated mesopores nature of the adsorbents as shown in Table 1. The surface areas of the freshly decomposed samples (Table 1) are 40 m^2/g, 48 m^2/g and 54 m^2/g for g-$Ca_{0.89}Mg_{0.1}O$, g-$Ca_{0.79}Mg_{0.2}O$ and g-$Ca_{0.69}Mg_{0.3}O$ respectively, which are the highest values reported so far for CaO based sorbents (about 5-45 m^2/g)[51],[52].

Table 1. BET surface area, pore volume and pore diameter for g-$Ca_{0.89}Mg_{0.1}O$, g-$Ca_{0.79}Mg_{0.2}O$ and g-$Ca_{0.69}Mg_{0.3}O$ samples.

Sample	S_{BET} (m^2g^{-1})	Pore volume (cm^3g^{-1})	Pore diameter (nm)
g-$Ca_{0.89}Mg_{0.1}O$	40	0.091	9.3
g-$Ca_{0.79}Mg_{0.2}O$	48	0.105	8.9
g-$Ca_{0.69}Mg_{0.3}O$	54	0.113	8.5

3.2. CO_2 capture and cycling studies

CO_2 capture studies were carried out by equilibrating the freshly prepared MMO sorbents with 86 % and 14 % CO_2 at 650 °C for 120 minutes, as explained in the experimental section. Carbonation efficiency of the MMO along with estimated amounts of carbon, MgO and CaO for all the three MMO are listed in Table 2. Amount of Mg and Ca in the MMO sorbents were estimated post decomposition of the metal-adamantanecarboxylates precursors by ICP-OES analysis, and the percentage of MgO and CaO calculated are shown in Table 2. The expected carbonation efficiency of the samples was calculated based on the amount of CaO present in g-$Ca_{0.89}Mg_{0.1}O$, g-$Ca_{0.79}Mg_{0.2}O$ and g-$Ca_{0.69}Mg_{0.3}O$ sorbents. The CO_2 capture capacity measurements for all the MMO sorbents under 86 and 14 % CO_2 were carried out at

650 °C for 120 minutes and results are shown in SI, Figure S7 and S8 respectively. g-$Ca_{0.89}Mg_{0.1}O$, g-$Ca_{0.79}Mg_{0.2}O$ and g-$Ca_{0.69}Mg_{0.3}O$ sorbents sorbed 63.33, 58.79 and 53.03 wt % of CO_2 respectively under 86 % CO_2. While the same sorbents when equilibrated with 14 % CO_2 sorbed 62.4, 57.98 and 53.0 wt % of CO_2 respectively. Based on the amount of CaO present in each sample, the carbonation efficiency values calculated ranges from 96-98 % (Table 2) for carbonation under 14 % and 86 % CO_2. A general trend of increase in carbonation efficiency going from g-$Ca_{0.89}Mg_{0.1}O$ to g-$Ca_{0.69}Mg_{0.3}O$ sorbents observed can be attributed to the composition of the MMO. The carbonation efficiency values reported here (96-98 %) are comparable with the best (95 - 100 %) previously reported synthetic CaO based sorbents tested under similar conditions[18,42,49,50].

Table 2. Amount of carbon, MgO and CaO and carbonation efficiencies of the MMO sorbents at 650 °C, 120 min and atmospheric pressure.

Sample	C (wt %) [a]	MgO (wt %) [b]	CaO (wt %) [b]	Carbonation Efficiency (%) under 86 % CO_2	Carbonation Efficiency (%) under 14 % CO_2
g-$Ca_{0.89}Mg_{0.1}O$	9.28	7.39	83.33	97.4	96.07
g-$Ca_{0.79}Mg_{0.2}O$	7.46	15.20	77.34	97.6	96.12
g-$Ca_{0.69}Mg_{0.3}O$	7.24	23.30	69.46	97.9	97.84

[a] Determined by CHN analysis [b] Determined by ICP-OES analysis

The samples carbonated under 86 % CO_2 were analysed with PXRD for phase formation of the carbonate as shown in SI, Figure S9. The PXRD patterns of all the carbonated sorbents indicate the formation of $CaCO_3$ (calcite) due to the reflections observed at 2θ values of 21.41°, 29.38° (100 % peak), 36.06°, 39.46°, 43.14°, 47.40° and 48.46° corresponding to *d*-values of 4.14 Å, 3.03 Å, 2.49 Å, 2.28 Å, 2.09 Å, 1.91 Å and 1.87 Å respectively. Additional to these reflections, a broad hump due to graphitic carbon at 2θ, 18.72° (4.73 Å) also was observed. Absence of reflections related to $MgCO_3$ indicates the non-participation of MgO component in CO_2 capture under the experimental carbonation conditions.

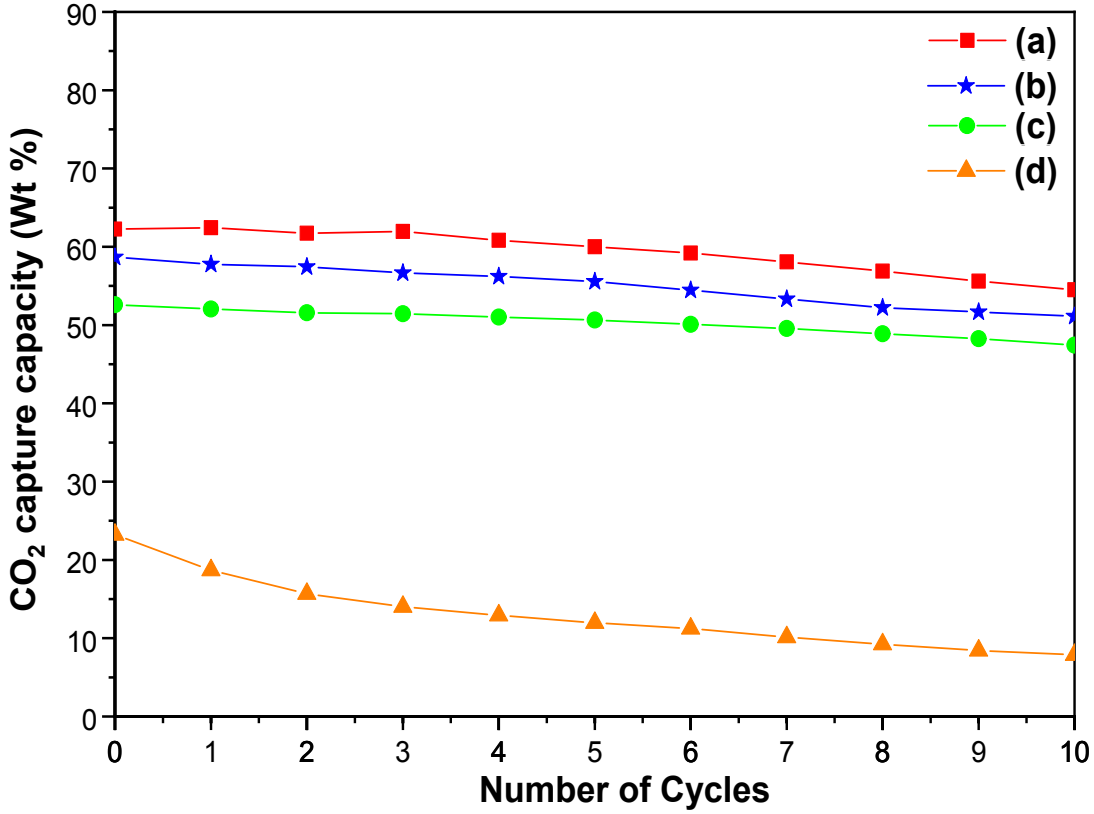

Figure 3. Cycling Studies of g-$Ca_{0.89}Mg_{0.1}O$ (a), g-$Ca_{0.79}Mg_{0.2}O$ (b), g-$Ca_{0.69}Mg_{0.3}O$ (c) and L-CaO (d). Carbonation was carried out at 650 °C, under 86% CO_2 (atmospheric pressure), and regeneration was carried out at 700 °C, under 100% N_2 (atmospheric pressure).

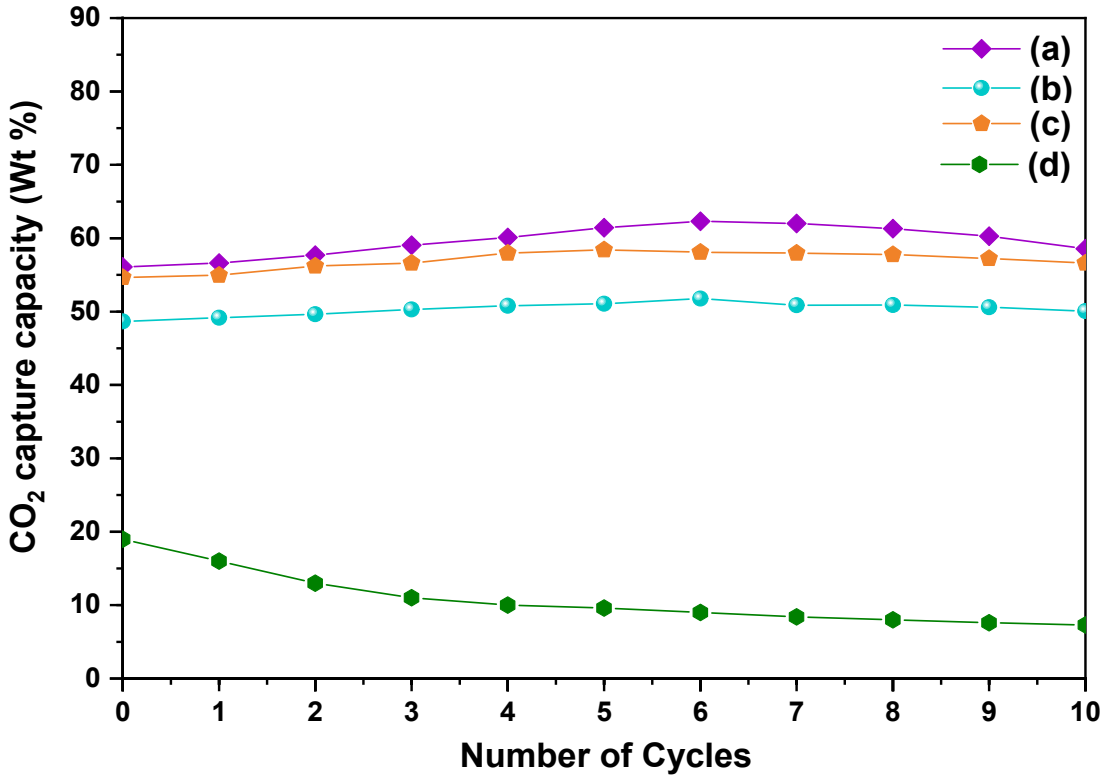

Figure 4. Cycling Studies of g-$Ca_{0.89}Mg_{0.1}O$ (a), g-$Ca_{0.79}Mg_{0.2}O$ (b), g-$Ca_{0.69}Mg_{0.3}O$ (c) and L-CaO (d). Carbonation was carried out at 650 °C, under 14% CO_2 (atmospheric pressure) and regeneration was carried out at 700 °C, under 100% N_2 (atmospheric pressure).

Table 3. Percentage loss in capture capacity of MMO sorbents with benchmark L-CaO sorbent under 86 % and 14 % CO_2 in 10 cycles.

Sample	Loss in capture capacity (%), 86 % CO_2, 10 cycles	Loss in capture capacity (%), 14 % CO_2, 10 cycles
g-$Ca_{0.89}Mg_{0.1}O$	12.38	5.52
g-$Ca_{0.79}Mg_{0.2}O$	12.15	3.06
g-$Ca_{0.69}Mg_{0.3}O$	9.27	1.09
L- CaO	65.19	61.29

Carbonation/regeneration studies of all the three sorbents were carried out under 86 % and 14 % CO_2 as described in the experimental section for 10 cycles. CO_2 capture capacities of sorbents under 86 % CO_2 are shown in Figure 3a, b and c respectively. The sample g-$Ca_{0.89}Mg_{0.1}O$, showed capture capacity of 62.35 wt % in the first cycle and retains close to 88 wt % initial capture capacity after 10 cycles. Similarly, g-$Ca_{0.79}Mg_{0.2}O$ shows 58.24 wt % capture capacity in the first cycle and retains 88 wt % of initial capture capacity as in the case of g-$Ca_{0.89}Mg_{0.1}O$. Finally, g-$Ca_{0.69}Mg_{0.3}O$ shows initial capture capacity 52.50 wt % and retains close to 91 wt % initial capture capacity after the 10 carbonation/regeneration cycles. All the three sorbents show slightly lower initial CO_2 capture capacity under 30 min equilibration time when compared to equilibrating the samples for 120 min as discussed above. Carbonation/regeneration cycling study of all the three sorbents under 14 % CO_2 (Figure 4a, b and c) showed a slightly different profile for CO_2 capture. All sorbents show an initial increase in the capture capacities until about the 6th cycle, followed by a gradual decay in the capture capacities. Initial capture capacities for g-$Ca_{0.89}Mg_{0.1}O$, g-$Ca_{0.79}Mg_{0.2}O$ and g-$Ca_{0.69}Mg_{0.3}O$ sorbents were found to be 56.16, 54.76 and 48.83 wt % respectively. The initial increase in the CO_2 capture capacities of a sorbent under 14 % CO_2 is described as the stabilisation of the carbonation process in various recent reports[54]. Therefore, the maximum amount of CO_2 captured (around the 6th cycle) for g-$Ca_{0.89}Mg_{0.1}O$, g-$Ca_{0.79}Mg_{0.2}O$ and g-$Ca_{0.69}Mg_{0.3}O$ sorbents under 14 % was found to be 62.23, 58.48 and 50.12 wt % respectively. The maximum CO_2 capture capacity value for each sample was used for calculation of percentage loss in capture capacity. g-$Ca_{0.89}Mg_{0.1}O$, g-$Ca_{0.79}Mg_{0.2}O$ and g-$Ca_{0.69}Mg_{0.3}O$ sorbents underwent 5.52, 3.06 and 1.09 % loss in their CO_2 capture capacities respectively under 14 % CO_2 as shown in Table 3. The average deactivation per carbonation /decarbonation cycle for a recently reported MgO - CaO synthetic sorbent was 0.42 %[44], in contrast to the g-$Ca_{0.69}Mg_{0.3}O$ sorbent that deactivates by 0.11 %. While optimised sample reported by Naeem et al under certain mild carbonation and regeneration cycles did not lose its carbon capture capacity in the first 10 cycles[19]. The performance of the synthetic MMO sorbents reported here are also compared with benchmark L-CaO sorbent under similar conditions. L-CaO showed CO_2 capture capacities of 22.82 and 18.78 wt % initial capture capacity under 86 and 14 % CO_2 as shown in Figure 3d and Figure 4d respectively. The sample losses considerable amount of capture at the end of 10 cycles (Table 3). The L-CaO retains only 34.8 and 38.7 % of its initial capture capacity under 86 and 14 % CO_2

respectively. The better CO_2 capture capacity of hydrothermally derived CaO based sorbents when compared to limestone derived CaO was also reported by Naeem et al[19].

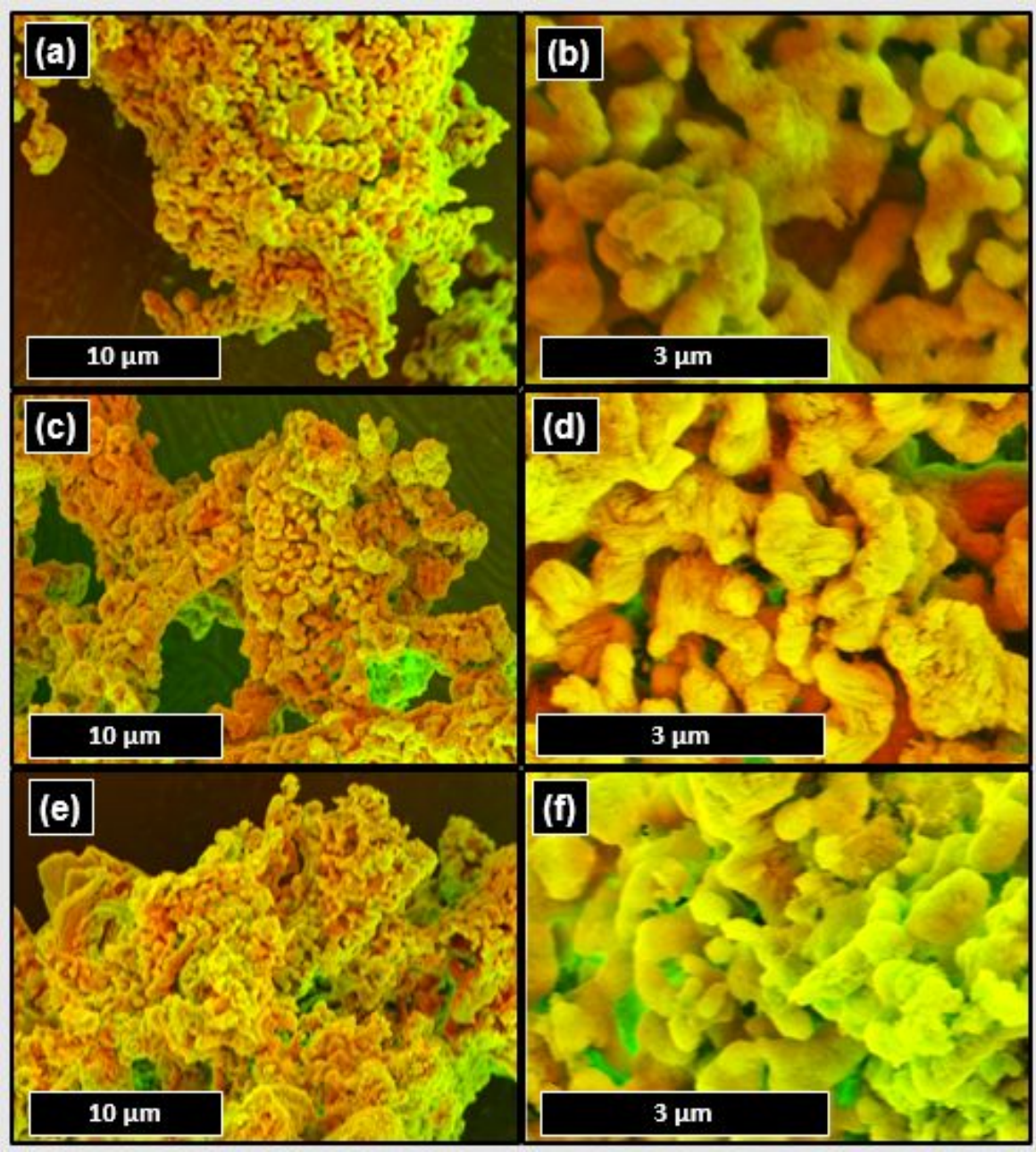

Figure 5. SEM images of g-$Ca_{0.89}Mg_{0.1}O$ (a, b), g-$Ca_{0.79}Mg_{0.2}O$ (c, d) and g-$Ca_{0.69}Mg_{0.3}O$ (e, f) sorbents obtained after 10 carbonation-regeneration cycles. Scalebars redrawn for clarity.

The MMO sorbents were analysed using SEM for any modification in structure/morphology following a series of 10 carbonation/regeneration cycles. The SEM images of the MMO sorbents, g-$Ca_{0.89}Mg_{0.1}O$, g-$Ca_{0.79}Mg_{0.2}O$ and g-$Ca_{0.69}Mg_{0.3}O$ are shown in Figure 5 (a, b), (c, d) and (e, f) respectively. The globular morphology of the freshly prepared MMO sorbents transform into yarns of micro-fibrous filaments stacked on the carbon support. The morphology indicates retention of sinter-free, macro-porous structure of the MMO sorbents after 10 carbonation/regeneration cycles which is vital to the low loss in the CO_2 capture capacity. Similar observation was made for synthetic carbon supported CaO samples reported recently[26].

All three MMO, despite having a common sinter-free carbon support, showed different behaviour upon cyclic carbonation/regeneration. Therefore, the amount of magnesium in the hydrothermally prepared Ca, Mg-adamantanecarboxylate precursor is also expected to have a role in stabilizing CaO from sintering. MgO has been reported to increase the stability of CaO sorbents[55]. Among the three compositions prepared, the g-$Ca_{0.69}Mg_{0.3}O$ sorbent exhibited the best carbonation efficiency and cycling performance, probably related to the better distribution of Mg in the oxide matrix, when compared to the other two sorbents, as discussed earlier. Moreover, higher percentages of Mg in the samples gave relatively smaller sized CaO, with MgO preventing the sintering of the CaO particles during repeated carbonation/regeneration cycles.

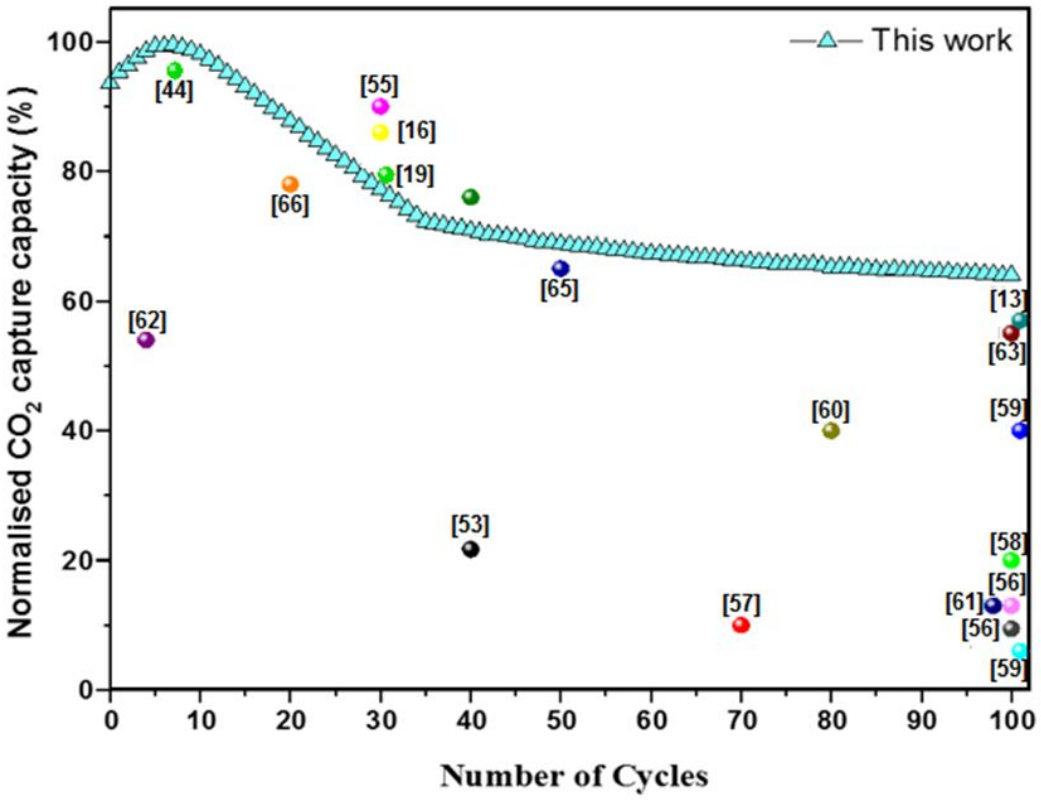

Figure 6. Normalised CO_2 capture capacity over 100 carbonation/regeneration cycles for the g-$Ca_{0.69}Mg_{0.3}O$ sorbent. Carbonation was carried out at 650 °C, under 14% CO_2 (atmospheric pressure) and regeneration was carried out at 700 °C, under 100% N_2 (atmospheric pressure). The numbers in the brackets correspond to the relevant reference study.

Shorter (5 min) carbonation/regeneration cycling studies were also carried out for the g-$Ca_{0.69}Mg_{0.3}O$ sorbent, as it showed the highest carbonation efficiency and lowest decay under 14 % CO_2. The sorbent showed an initial CO_2 capture capacity of 48.13 wt % (SI, Figure S10) that reached a maximum of 51.25 wt % (at around the 6th cycle), as in the previous case. After 10 consecutive carbonation/regeneration cycles, the sorbent showed a CO_2 capture capacity of 49.98 wt %. This value account for a carbonation efficiency of 94.6 % and the sample retained 98 % of its initial capture capacity.

In order to test the long-term cycling stability of the g-$Ca_{0.69}Mg_{0.3}O$ sorbent, carbonation/regeneration was extended for 100 cycles. A normalised CO_2 capture capacity graph of 100 cycles is shown in Figure 6. The CO_2 capture capacities retained after 'n'

number of carbonation/regeneration cycles for recently reported CaO samples are included in Figure 6 and listed in SI, Table S2, for comparison. The rate loss in capture capacity of the g-$Ca_{0.69}Mg_{0.3}O$ sorbent (shown in Figure 6) is faster from the 10th to around 30th cycle, and thereafter becomes more gradual. The CaO based sorbents reported recently also showed close to about 20 % loss in activity after 30 carbonation/regeneration cycles, as depicted in Figure 6[16,19,55]. In this case, after the 70th cycle, the g-$Ca_{0.69}Mg_{0.3}O$ sorbent showed stable cycling behaviour with minimal activity loss. Even more, upon completion of 100 cycles, the sample retained 64.2 % of its initial CO_2 capture capacity, in contrast to other CaO based sorbents that retained between 9 % to 57 % of their initial values, as shown in Figure 6 and Table S2 (SI).

4. Conclusions

Here we report a facile green synthesis method to produce carbon supported MgO stabilised CaO sorbents, their high temperature CO_2 capture and cycling studies. The Ca, Mg-adamantanecarboxylates were synthesized by employing just the required amounts of metal hydroxides and 1-adamantanecarboxylic acid. No excess chemicals were used and the synthesis method does not involve post synthesis washing. The Ca : Mg ratio in the samples was varied (9, 4 and 2.33) to get the optimum composition. The as synthesized precursor samples were decomposed under inert atmosphere to get the carbon supported MgO stabilized CaO MMO. The adamantanecarboxylate ion used in the synthesis was converted to graphitic carbon upon thermal decomposition and acts as a support for the resultant MMO sorbents. Among all the samples, g-$Ca_{0.69}Mg_{0.3}O$ sorbent with a Ca : Mg ratio of about 2.33 shows better distribution of MgO over others. All the sorbents show better CO_2 capture and cycling performance compared to the limestone derived CaO under both, CO_2 rich and lean conditions. A carbonation efficiency ranging from 96 to 98 % was achieved for all the samples. Sorbents retained between 88 to 99 % of its initial capture capacity after 10 carbonation/regeneration cycles when exposed to 86 % and 14 % CO_2 gaseous mixtures. The carbonation efficiency and cycling stability increases with increasing amount of MgO present in the sample. Thus, the g-$Ca_{0.69}Mg_{0.3}O$ sorbent, which contained the highest amount and best distribution of Mg, showed a better stability and resistance to loss in CO_2 capture capacity in comparison to the other two sorbents. The g-$Ca_{0.69}Mg_{0.3}O$ sorbent showed close to 95 %

carbonation efficiency and retained about 65 % of initial CO_2 capture capacity after 100 cycles of 5 minutes each under 14 % CO_2.

Associated Content

Supporting Information (SI) file contains: elemental analysis (Table S1), FTIR spectrum (Figure S1), PXRD patterns (Figure S2) of Ca, Mg-Adamantanecarboxylate precursor samples, N_2 adsorption isotherms (Figure S3), elemental maps of the developed sorbents (Figure S4, S5 and S6), CO_2 adsorption isotherms in 86 % CO_2 (Figure S7) and 14 % CO_2 (Figure S8) carried out for 2 hours, PXRD patterns of the carbonated sorbents in 86 % CO_2 (Figure S9), 5 min cyclic carbonation/regeneration cycles of g-$Ca_{0.69}Mg_{0.3}O$ sorbent under 14 % CO_2 (Figure S10) and literature reports of CaO based sorbents with CO_2 capture capacities after 'n' carbonation/regeneration cycles (Table S2).

Acknowledgements

The authors acknowledge the financial support from EPSRC through grants EP/N024540/1 and EP/N009924/1, as well as the Buchan Chair in Sustainable Energy Engineering.

References

(1) Mac Dowell, N.; Fennell, P. S.; Shah, N.; Maitland, G. C. The Role of CO2 Capture and Utilization in Mitigating Climate Change. *Nat. Clim. Chang.* **2017**, *7* (4), 243–249. https://doi.org/10.1038/nclimate3231.

(2) Fernández, J. R.; Garcia, S.; Sanz-Pèrez, E. S. CO_2 Capture and Utilization. *Ind. Eng. Chem. Res.* **2020**, *59*, 6767–6772. https://doi.org/https://dx.doi.org/10.1021/acs.iecr.0c01643.

(3) D'Alessandro, D. M.; Smit, B.; Long, J. R. Carbon Dioxide Capture: Prospects for New Materials. *Angewandte Chemie - International Edition*. 2010. https://doi.org/10.1002/anie.201000431.

(4) Rochelle, G. T. Amine Scrubbing for CO2 Capture. *Science*. 2009. https://doi.org/10.1126/science.1176731.

(5) D'Alessandro, D. M.; Smit, B.; Long, J. R. Carbon Dioxide Capture: Prospects for

New Materials. *Angew. Chemie Int. Ed.* **2010**, *49* (35), 6058–6082. https://doi.org/10.1002/anie.201000431.

(6) Gupta, H.; Fan, L. S. Carbonation-Calcination Cycle Using High Reactivity Calcium Oxide for Carbon Dioxide Separation from Flue Gas. *Ind. Eng. Chem. Res.* **2002**, *41* (16), 4035–4042. https://doi.org/10.1021/ie010867l.

(7) Wang, S.; Yan, S.; Ma, X.; Gong, J. Recent Advances in Capture of Carbon Dioxide Using Alkali-Metal-Based Oxides. *Energy Environ. Sci.* **2011**, *4* (10), 3805–3819. https://doi.org/10.1039/c1ee01116b.

(8) Adánez, J.; De Diego, L. F.; García-Labiano, F.; Gayán, P.; Abad, A.; Palacios, J. M. Selection of Oxygen Carriers for Chemical-Looping Combustion. *Energy and Fuels* **2004**, *18* (2), 371–377. https://doi.org/10.1021/ef0301452.

(9) Lin, Y.; Kong, C.; Zhang, Q.; Chen, L. Metal-Organic Frameworks for Carbon Dioxide Capture and Methane Storage. *Advanced Energy Materials*. 2017. https://doi.org/10.1002/aenm.201601296.

(10) Liu, M.; Gurr, P. A.; Fu, Q.; Webley, P. A.; Qiao, G. G. Two-Dimensional Nanosheet-Based Gas Separation Membranes. *J. Mater. Chem. A* **2018**, *6* (46), 23169–23196. https://doi.org/10.1039/C8TA09070J.

(11) Gadipelli, S.; Howard, C. A.; Guo, J.; Skipper, N. T.; Zhang, H.; Shearing, P. R.; Brett, D. J. L. Superior Multifunctional Activity of Nanoporous Carbons with Widely Tunable Porosity: Enhanced Storage Capacities for Carbon-Dioxide, Hydrogen, Water, and Electric Charge. *Adv. Energy Mater.* **2020**, *1903649*, 1–14. https://doi.org/10.1002/aenm.201903649.

(12) MacDowell, N.; Florin, N.; Buchard, A.; Hallett, J.; Galindo, A.; Jackson, G.; Adjiman, C. S.; Williams, C. K.; Shah, N.; Fennell, P. An Overview of CO2 Capture Technologies. *Energy and Environmental Science*. 2010. https://doi.org/10.1039/c004106h.

(13) Li, L.; King, D. L.; Nie, Z.; Li, X. S.; Howard, C. MgAl2O4 Spinel-Stabilized Calcium Oxide Absorbents with Improved Durability for High-Temperature CO2 Capture. *Energy and Fuels* **2010**, *24* (6), 3698–3703. https://doi.org/10.1021/ef100245q.

(14) Valverde, J. M. Ca-Based Synthetic Materials with Enhanced CO2 Capture Efficiency. *J. Mater. Chem. A* **2013**, *1* (3), 447–468. https://doi.org/10.1039/c2ta00096b.

(15) Stanmore, B. R.; Gillet, P. Review-Calcination And Carbonation of Limestone During Thermal Cycling For CO2 Sequestration. *Fuel Process. Technol.* **2005**, *86*, 1707–1743. https://doi.org/10.1016/j.fuproc.2005.01.023

(16) Li, Z. S.; Cai, N. S.; Huang, Y. Y. Effect of Preparation Temperature on Cyclic CO2 Capture and Multiple Carbonation-Calcination Cycles for a New Ca-Based CO2 Sorbent. *Ind. Eng. Chem. Res.* **2006**, *45* (6), 1911–1917. https://doi.org/10.1021/ie0512111.

(17) Hughes, R. W.; Lu, D.; Anthony, E. J.; Wu, Y. Improved Long-Term Conversion of Limestone-Derived Sorbents for in Situ Capture of CO2 in a Fluidized Bed Combustor. *Ind. Eng. Chem. Res.* **2004**, *43* (18), 5529–5539. https://doi.org/10.1021/ie034260b.

(18) Feng, B.; Liu, W.; Li, X.; An, H. Overcoming the Problem of Loss-in-Capacity of Calcium Oxide in CO2 Capture. *Energy and Fuels* **2006**, *20* (6), 2417–2420. https://doi.org/10.1021/ef060258w.

(19) Naeem, M. A.; Armutlulu, A.; Imtiaz, Q.; Donat, F.; Schäublin, R.; Kierzkowska, A.; Müller, C. R. Optimization of the Structural Characteristics of CaO and Its Effective Stabilization Yield High-Capacity CO2 Sorbents. *Nat. Commun.* **2018**, *9* (1), 1–11. https://doi.org/10.1038/s41467-018-04794-5.

(20) Manovic, V.; Anthony, E. J. CaO-Based Pellets Supported by Calcium Aluminate Cements for High-Temperature CO2 Capture. *Environ. Sci. Technol.* **2009**, *43* (18), 7117–7122. https://doi.org/10.1021/es901258w.

(21) Ping, H.; Wu, S. CO2 Sorption Durability of Zr-Modified Nano-CaO Sorbents with Cage-like Hollow Sphere Structure. *ACS Sustain. Chem. Eng.* **2016**, *4* (4), 2047–2055. https://doi.org/10.1021/acssuschemeng.5b01397.

(22) Ping, H.; Wang, Y.; Wu, S. Preparation of MgO-Coated Nano CaO Using Adsorption Phase Reaction Technique for CO2 Sorption. *RSC Adv.* **2016**, *6* (47), 41239–41246. https://doi.org/10.1039/c6ra05452h.

(23) Gunathilake, C.; Jaroniec, M. Mesoporous Calcium Oxide-Silica and Magnesium Oxide-Silica Composites for CO2 Capture at Ambient and Elevated Temperatures. *J. Mater. Chem. A* **2016**, *4* (28), 10914–10924. https://doi.org/10.1039/c6ta03916b.

(24) Derevschikov, V. S.; Lysikov, A. I.; Okunev, A. G. High Temperature CaO/Y2O3 Carbon Dioxide Absorbent with Enhanced Stability for Sorption-Enhanced Reforming Applications. *Ind. Eng. Chem. Res.* **2011**, *50* (22), 12741–12749. https://doi.org/10.1021/ie2015334.

(25) Mahinpey, N.; Sedghkerdar, M. H.; Aqsha, A.; Soleimanisalim, A. H. CO2 Capture Performance of Core/Shell CaO-Based Sorbent Using Mesostructured Silica and Titania in a Multicycle CO2 Capture Process. *Ind. Eng. Chem. Res.* **2016**, *55* (16), 4532–4538. https://doi.org/10.1021/acs.iecr.6b00469.

(26) Manohara, G. V.; Maroto-Valer, M.; Garcia, S. A Simple and Green Synthesis Method for Ca-Adamantanecarboxylate: A Novel Precursor for High Temperature CO2 Capture Sorbent Materials. *Sustain. Energy Fuels* **2019**, *3* (12), 3318–3323. https://doi.org/10.1039/c9se00451c.

(27) Wu, Z.; Hao, N.; Xiao, G.; Liu, L.; Webley, P.; Zhao, D. One-Pot Generation of Mesoporous Carbon Supported Nanocrystalline Calcium Oxides Capable of Efficient CO2 Capture over a Wide Range of Temperatures. *Phys. Chem. Chem. Phys.* **2011**, *13* (7), 2495–2503. https://doi.org/10.1039/c0cp01807d.

(28) Lewalska-Graczyk, A.; Pieta, P.; Garbarino, G.; Busca, G.; Holdynski, M.; Kalisz, G.; Sroka-Bartnicka, A.; Nowakowski, R.; Naushad, M.; Gawande, M. B.; Zbořil, R.; Pieta, I. S. Graphitic Carbon Nitride–Nickel Catalyst: From Material Characterization to Efficient Ethanol Electrooxidation. *ACS Sustain. Chem. Eng.* **2020**, *8* (18), 7244–7255. https://doi.org/10.1021/acssuschemeng.0c02267.

(29) Nityashree, N.; Price, C. A. H.; Pastor-Perez, L.; Manohara, G. V.; Garcia, S.; Maroto-Valer, M. M.; Reina, T. R. Carbon Stabilised Saponite Supported Transition Metal-Alloy Catalysts for Chemical CO2 Utilisation via Reverse Water-Gas Shift Reaction. *Appl. Catal. B Environ.* **2020**, *261* (September 2019). https://doi.org/10.1016/j.apcatb.2019.118241.

(30) Manohara, G. V.; Maroto-Valer, M. M.; Garcia, S. The Effect of the Layer-Interlayer Chemistry of LDHs on Developing High Temperature Carbon Capture Materials. *Dalt. Trans.* **2020**, *49* (3), 923–931. https://doi.org/10.1039/c9dt03913a.

(31) Garcia-Gallastegui, A.; Iruretagoyena, D.; Gouvea, V.; Mokhtar, M.; Asiri, A. M.; Basahel, S. N.; Al-Thabaiti, S. A.; Alyoubi, A. O.; Chadwick, D.; Shaffer, M. S. P. Graphene Oxide as Support for Layered Double Hydroxides: Enhancing the CO2 Adsorption Capacity. *Chem. Mater.* **2012**, *24* (23), 4531–4539. https://doi.org/10.1021/cm3018264.

(32) Li, P.; Zeng, H. C. Hierarchical Nanocomposite by the Integration of Reduced Graphene Oxide and Amorphous Carbon with Ultrafine MgO Nanocrystallites for Enhanced CO2 Capture. *Environ. Sci. Technol.* **2017**, *51* (21), 12998–13007. https://doi.org/10.1021/acs.est.7b03308.

(33) Zhou, Z.; Qi, Y.; Xie, M.; Cheng, Z.; Yuan, W. Synthesis of CaO-Based Sorbents through Incorporation of Alumina/Aluminate and Their CO 2 Capture Performance. *Chem. Eng. Sci.* **2012**, *74*, 172–180. https://doi.org/10.1016/j.ces.2012.02.042.

(34) Tomkute, V.; Solheim, A.; Olsen, E. Investigation of High-Temperature CO2 Capture by CaO in CaCl2 Molten Salt. *Energy and Fuels* **2013**, *27* (9), 5373–5379. https://doi.org/10.1021/ef4009899.

(35) Anbia, M.; Hoseini, V. Development of MWCNT@MIL-101 Hybrid Composite With Enhanced Adsorption Capacity For Carbon Dioxide. *Chem. Eng. J.* **2012**, *191*, 326–330. https://doi.org/10.1016/j.cej.2012.03.025.

(36) Lu, H.; Khan, A.; Pratsinis, S. E.; Smirniotis, P. G.; Zu, C.-. Flame-Made Durable Doped-CaO Nanosorbents for CO2 Capture. *Energ. Fuel.* **2009**, *96* (16), 1093–1100. https://doi.org/10.1021/ef8007882.

(37) Radfarnia, H. R.; Sayari, A. Highly Efficient CaO-Based CO_2 Sorbent Prepared by a Citrate-Assisted Sol-Gel Technique. *Chem. Eng. J.* **2015**, *262*, 913–920. https://doi.org/10.1016/j.cej.2014.09.074.

(38) Pichardo, A. G.; Correa, F. G.; Mendieta, V. S.; Mendosa, H. H. New CaO-Based Adsorbents Prepared by Solution Combustion and High-Energy Ball-Milling Process

for CO2 Adsorption: Textural and Structural Influences. *Arab. J. Chem.* **2020**, *13*, 171–183. https://doi.org/10.1016/j.arabjc.2017.03.005.

(39) Al-Jeboori, M. J.; Fennell, P. S.; Nguyen, M.; Feng, K. Effects of Different Dopants and Doping Procedures on the Reactivity of CaO-Based Sorbents for CO2 Capture. *Energy and Fuels* **2012**, *26* (11), 6584–6594. https://doi.org/10.1021/ef301153b.

(40) Narayanappa, A. N.; Kamath, P. V. Interaction of Pristine Hydrocalumite-Like Layered Double Hydroxides with Carbon Dioxide. *ACS Omega* **2019**, *4* (2), 3198–3204. https://doi.org/10.1021/acsomega.9b00083.

(41) Manohara, G. V.; Kunz, D. A.; Kamath, P. V.; Milius, W.; Breu, J. Homogeneous Precipitation by Formamide Hydrolysis: Synthesis, Reversible Hydration, and Aqueous Exfoliation of the Layered Double Hydroxide (LDH) of Ni and Al. *Langmuir* **2010**, *26* (19), 15586–15591. https://doi.org/10.1021/la103108f.

(42) Dou, B.; Wang, C.; Song, Y.; Chen, H.; Jiang, B.; Yang, M.; Xu, Y. Solid Sorbents for In-Situ CO2 removalDuring Sorption-Enhanced Steam Reforming Process: A Review. *Renew. Sustain. Energy Rev.* **2016**, *53*, 536–546. https://doi.org/10.1016/j.rser.2015.08.068.

(43) Zhu, Q.; Zeng, S.; Yu, Y. A Model to Stabilize CO2 Uptake Capacity during Carbonation-Calcination Cycles and Its Case of CaO-MgO. *Environ. Sci. Technol.* **2017**, *51* (1), 552–559. https://doi.org/10.1021/acs.est.6b04100.

(44) Huang, L.; Zheng, Q.; Louis, B.; Wang, Q. A Facile Solvent/Nonsolvent Preparation of Sintering-Resistant MgO/CaO Composites for High-Temperature CO2 Capture. *Energy Technol.* **2018**, *6* (12), 2469–2478. https://doi.org/10.1002/ente.201800300.

(45) Bhatta, L. K. G.; Subramanyam, S.; Chengala, M. D.; Olivera, S.; Venkatesh, K. Progress In Hydrotalcite Like Compounds And Metal-Based Oxides For CO2 Capture: A Review. *J. Clean. Prod.* **2015**, *103*, 171–196. https://doi.org/10.1016/j.clepro.2014.12.059.

(46) Manohara, G.V.; Greenwell, H. C.; Alabedi, G. S.; Hall, J. A.; Whiting, A. Synthesis Of Magnesium Adamantane Salts And Magnesium Oxide Nanocomposites , And Systems And Methods Including The Salts Or The Nanocomposites, **2018**,

US10106482B2.

(47) Nakamoto, K. *Infrared and Raman Spectra of Inorganic and Coordination Compounds: Part A: Theory and Applications in Inorganic Chemistry: Sixth Edition*; 2008. https://doi.org/10.1002/9780470405840.

(48) Wang, Q.; Zhang, Q.; Chen, L.; Yu, L.; Dong, L. A Simple Method to Synthesize Multi-Branched Carbon Fibers Using Cuppric Chloride Aqueous Soulution as Catalyst Precursor. *J. Mater. Sci. Technol.* **2014**, *30* (9), 917–921. https://doi.org/10.1016/j.jmst.2013.10.019.

(49) Martavaltzi, C. S.; Lemonidou, A. A. Parametric Study of the CaO-Ca12Al14O33 Synthesis with Respect to High CO2 Sorption Capacity and Stability on Multicycle Operation. *Ind. Eng. Chem. Res.* **2008**, *47* (23), 9537–9543. https://doi.org/10.1021/ie800882d.

(50) Thommes, M.; Kaneko, K.; Neimark, A. V.; Olivier, J. P.; Rodriguez-Reinoso, F.; Rouquerol, J.; Sing, K. S. W. Physisorption of Gases, with Special Reference to the Evaluation of Surface Area and Pore Size Distribution (IUPAC Technical Report). *Pure Appl. Chem.* **2015**, *87* (9–10), 1051–1069. https://doi.org/10.1515/pac-2014-1117.

(51) Hlaing, N. N.; Vignesh, K.; Sreekantan, S.; Pung, S. -Y.; Hinode, H.; Kurniawa, W.; Othman, R.; Thant, A. A.; Mohamed, A. R.; Salim, C. Effect of Cetyl Trimethyl Ammonium Bromide on Structure, Morphology Carbon Dioxide Adsorption Capacity of Calcium Hydroxide Based Sorbents. *Appl. Surf. Sci.* **2016**, *363*, 586–592. https://doi.org/10.1016/j.apsusc.2015.12.121.

(52) Hlaing, N. N.; Sreekantan, S.; Othman, R.; Pung, S. Y.; Hinode, H.; Kurniawan, W.; Thant, A. A.; Mohamed, A. R.; Salime, C. Sol-Gel Hydrothermal Synthesis of Microstructured CaO-Based Adsorbents for CO2 Capture. *RSC Adv.* **2015**, *5* (8), 6051–6060. https://doi.org/10.1039/c4ra14355h.

(53) Abanades, J. C.; Alvarez, D. Conversion Limits in the Reaction of CO2 with Lime. *Energy and Fuels* **2003**, *17* (2), 308–315. https://doi.org/10.1021/ef020152a.

(54) Manovic, V.; Anthony, E. J. Thermal Activation of CaO-Based Sorbent and Self-

Reactivation during CO2 Capture Looping Cycles. *Environ. Sci. Technol.* **2008**, *42* (11), 4170–4174. https://doi.org/10.1021/es800152s.

(55) Sánchez Jiménez, P. E.; Perejón, A.; Benítez Guerrero, M.; Valverde, J. M.; Ortiz, C.; Pérez Maqueda, L. A. High-Performance and Low-Cost Macroporous Calcium Oxide Based Materials for Thermochemical Energy Storage in Concentrated Solar Power Plants. *Appl. Energy* **2019**, *235*, 543–552. https://doi.org/10.1016/j.apenergy.2018.10.131.

(56) Alvarez, D.; Abanades, J. C. Pore-Size and Shape Effects on the Recarbonation Performance of Calcium Oxide Submitted to Repeated Calcination/Recarbonation Cycles. *Energy and Fuels* **2005**, *19* (1), 270–278. https://doi.org/10.1021/ef049864m.

(57) Curran, G. P.; Fink, C. E.; Gorin. E. CO2 Acceptor Gasification Process in *Fuel Gasification*. American Chemical Society, **1967**. Chapter 10,141–165. https://doi.org/10.1021/ba-1967-0069.ch010.

(58) Florin, N. H.; Harris, A. T. Reactivity of CaO Derived From Nano-Sized CaCO3 particles Through Mutiple CO2 Capture-And-Release Cycles. *Chem. Eng. Sci.* **2009**, *64*, 187–191. https://doi.org/10.1016/j.ces.2008.10.021.

(59) Lysikov, A. I.; Salanov, A. N.; Okunev, A. G. Change of CO2 Carrying Capacity of CaO in Isothermal Recarbonation-Decomposition Cycles. *Ind. Eng. Chem. Res.* **2007**, *46* (13), 4633–4638. https://doi.org/10.1021/ie0702328.

(60) Sanchez-Jimenez, P. E.; Perez-Maqueda, L. A.; Valverde, J. M. Nanosilica Supported CaO: A Regenerable and Mechanically Hard CO2 Sorbent at Ca-Looping Conditions. *Appl. Energy* **2014**, *118*, 92–99. https://doi.org/10.1016/j.apenergy.2013.12.024.

(61) Alonso, M.; Arias, B.; Fernández, J. R.; Bughin, O.; Abanades, C. Measuring Attrition Properties of Calcium Looping Materials in a 30 kW Pilot Plant. *Powder Technology*. 2018, pp 273–281. https://doi.org/10.1016/j.powtec.2018.06.011.

(62) André, L.; Abanades, S. Evaluation and Performances Comparison of Calcium, Strontium and Barium Carbonates during Calcination/Carbonation Reactions for Solar Thermochemical Energy Storage. *Journal of Energy Storage*. 2017, pp 193–205. https://doi.org/10.1016/j.est.2017.07.014.

(63) Koirala, R.; Gunugunuri, K. R.; Smirniotis, P. Effect of Zirconia Doping on Calcium Oxide on Stability and Performance during the Extended Operating Cycles. *Sep. Div. - Core Program. Top. 2011 AIChE Annu. Meet.* **2011**, *1*, 235.

(64) Wu, S. F.; Zhu, Y. Q. Behavior of CaTiO3/Nano-CaO as a CO2 Reactive Adsorbent. *Ind. Eng. Chem. Res.* **2010**, *49* (6), 2701–2706. https://doi.org/10.1021/ie900900r.

(65) Zhao, M.; Yang, X.; Church, T. L.; Harris, A. T. Novel CaO-SiO 2 Sorbent and Bifunctional Ni/Co-CaO/SiO 2 Complex for Selective H 2 Synthesis from Cellulose. *Environ. Sci. Technol.* **2012**, *46* (5), 2976–2983. https://doi.org/10.1021/es300135d.

(66) Luo, C.; Zheng, Y.; Ding, N.; Wu, Q.; Bian, G.; Zheng, C. Development and Performance of CaO/La2O3 Sorbents during Calcium Looping Cycles for CO2 Capture. *Ind. Eng. Chem. Res.* **2010**, *49* (22), 11778–11784. https://doi.org/10.1021/ie1012745.

Graphical Abstract

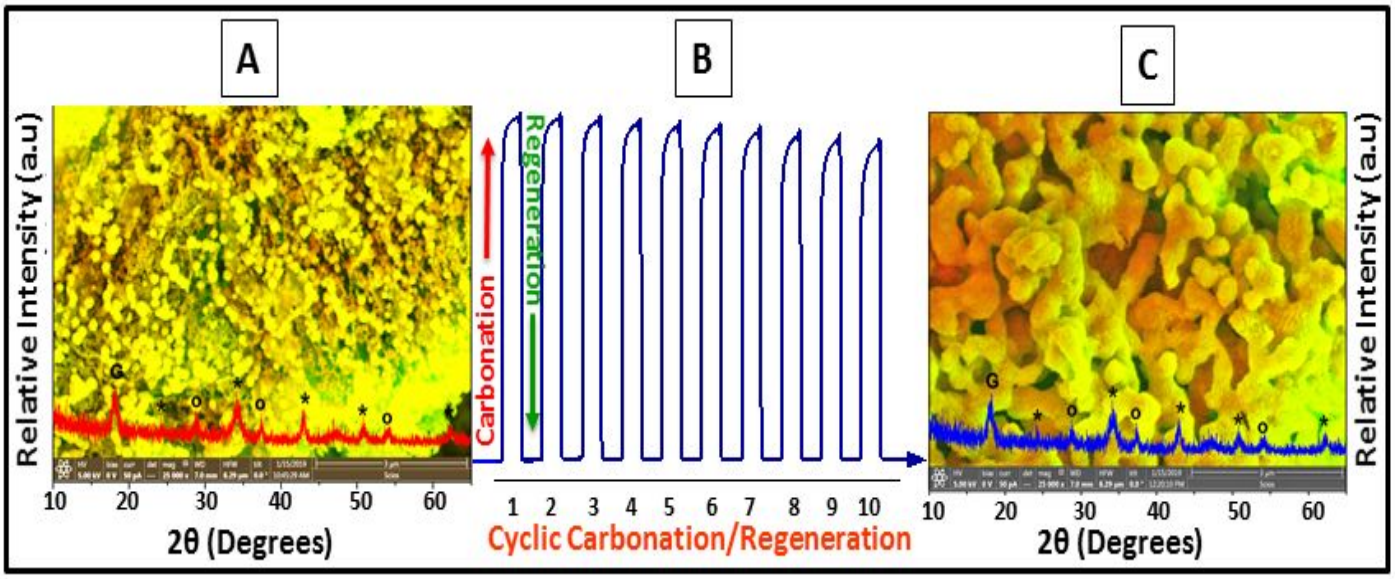

Scanning Electron Microscope images with embedded PXRD patterns of freshly prepared sorbent (A) and cycled sorbent (C) after 10 carbonation/regeneration cycles (B).

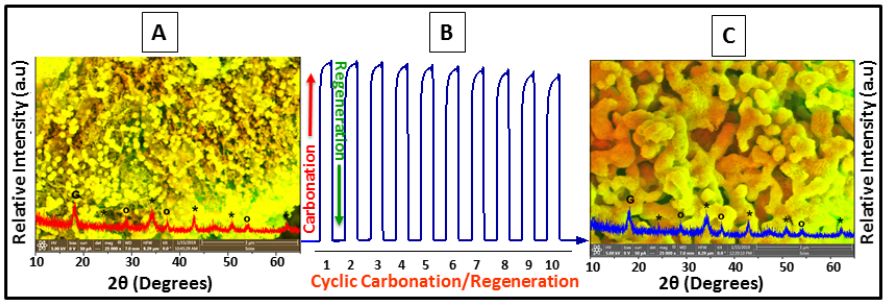

Scanning Electron Microscope images with embedded PXRD patterns of freshly prepared sorbent (A) and cycled sorbent (C) after 10 carbonation/regeneration cycles (B).

254x190mm (96 x 96 DPI)